Supporting Information

A Facile One-pot Strategy to Functionalize Graphene Oxide with Poly(amino-phosphonic acid) Derived from Wasted Acrylic Fibers for Effective Gd(III) Capture

Weiyan Yin[a*], Xinyu Zhan[a], Pai Fang[a], Minggui Xia[a*], Junxia Yu[b], Ru-an Chi[b*]

[a] Hubei Key Laboratory of Biomass Fibers and Eco-dyeing & Finishing, School of Chemistry and Chemical Engineering, Wuhan Textile University, No.1,Yangguang avenue, Wuhan 430073, China

[b] Xingfa School of Mining Engineering, Wuhan Institute of Technology, No.206, Guanggu 1st road, Wuhan 430074, China

[*]Corresponding authors.

Email: hpywy2006@163.com (Weiyan Yin).

Email: mingguixia1@163.com (Minggui Xia).

Email: rac_wit@163.com (Ru-an Chi).

Supporting information consists of 13 pages, 4 figures and 1 Table

SI. Preparation of adsorbent materials

SI-1. Preparation of MGO

Firstly, the GO was synthesized by a modified Hummers method [1]. In brief, natural flake graphite powder was oxidized by concentrated H_2SO_4 and $KMnO_4$ under ice bath condition with vigorous stirring. Followed by the addition of 30% H_2O_2 to eliminate the excess MnO_4^-. Subsequently, the preparation of MGO was performed by coprecipitation of Fe_3O_4 nanoparticles on the surface of GO sheets. Typically, Fe^{2+} and Fe^{3+} (molar ratio 1:2) were mixed in the GO solution under oxygen-free condition with addition of ammonia solution to prepare MGO.

SI-2. Preparation of PAPA, PAMGO-1, PAMGO-2, PAMGO-3, and PAMGO-4

A facile but effective one-pot reaction approach was used to prepare PAPA and PAMGOs. First, WAFs (1.0 g) was dispersed into DMF (50 mL), then added phosphorous acid (3.0 g) to the mixture, followed by refluxing for 14 h to form PAPA solution [2], the PAPA was got by precipitating in double distilled water. Thereafter, EDC (0.45 g), NHS (0.45 g) and MGO (1.0 g) were added to PAPA solution, and the mixture was vigorously stirred for 12 h at 85 ˚C to produce the PAMGOs (PAMGO-1, PAMGO-2 and PAMGO-3, and PAMGO-4) with different dosages of PAPA. Concisely, PAPA solution containing 0.5, 1.0, 2.0, and 5.0 g of WAFs were mixed NHS (0.45 g), EDC (0.45 g) and MGO (1.0 g) to obtain PAMGO-1, PAMGO-2, PAMGO-3 and PAMGO-4, respectively. Finally, the desired products were gathered by magnetic separation, and washed with DMF and double distilled water.

SII. Characterization of materials

The morphology of the samples were characterized by scanning electron microscopy (SEM, Zeiss Supra55). Powder X-ray diffraction (XRD) measurements were performed on X-ray diffraction analyzer (Bruker D8 Advance, Germany) using a Cu-Ka radiation (λ = 1.5406 Å) from the 2θ range of 5-80°. The specific surface area and pore-size distribution of the materials were recorded using an ASAP2010 (Micromeritics Inc., USA) BET-BJH instrument at 77 K within the P/P0 range of 0.05-0.2. The samples were degassed at 120 °C for 4 h under vacuum prior to the N_2 adsorption/desorption measurements. The zeta potentials of the samples were measured on a Malvern ZEN2600 Zetasizer. Fourier transform infrared spectra (FTIR) were recorded on an AVATAR 360 spectrometer (Nicolet, USA) using the KBr disk method within the range of 4000−400 cm^{-1}. Thermogravimetrical analyses (TGA) of the materials were carried out using a PerkinElmer 1061608 instrument within a temperature range of 25-800 ˚C at heating rate of 10 ˚C/min in nitrogen. Elemental analysis was carried out with an EA 1108 Fisons instruments through a dynamic flash combustion method. The concentrations of metal ions were determined with inductively coupled plasma optical emission spectrometer (ICP) (ICP2060T, Jiangsu Skyray Instrument Co. Ltd, China). X-ray photoelectron spectroscopy (XPS) measurements were carried out by a Thermo VG Multilab 2000 spectrometer with an Al Ka X-ray source.

SIII. Adsorption experiments

SIII-1. Adsorption equilibrium and removal efficiency measurement

The equilibrium adsorption capacity (q_e) and removal efficiency (RE) were calculated according to the Eq. (S1) and Eq. (S2):

$$q_e = \frac{(C_0 - C_e) \times V}{m} \quad \text{（S1）}$$

$$\text{Removal}(\%) = \frac{(C_0 - C_e)}{C_0} \times 100 \quad \text{（S2）}$$

Where C_0 and C_e are the initial and equilibrium concentrations of Gd(III) ions (mg/L), V (L) and m (g) represent volume of the solution and the weight of adsorbent.

SIII-2. Determination of adsorption selectivity:

The affinities of the adsorbents towards a given metal ion were estimated by the distribution coefficient value (K_D, mL/g) calculated using the following equation [3]:

$$K_D = \frac{(C_0 - C_e) \times V}{mC_e} \quad \text{(S3)}$$

Where C_0 is the initial metal ion concentration in the aqueous solution (mg/L), C_e is the final metal ion concentration in the aqueous solution (mg/L), V is the volume of the solution (mL), and m is the mass of the adsorbent (g).

SIII-3. Adsorption data fitting by isotherm models:

The Langmuir model is usually employed to describe a monolayer sorption onto a homogeneous surface of the adsorbent with identical binding sites. For Freundlich model, which is based upon the hypothesis that multilayer sorption arises on

heterogeneous systems. While the Temkin isotherm model assumes that the energy of the adsorption decreases with increasing the coverage of adsorption sites with adsorbate. The three models are simplified to the following linear forms [4-6], respectively.

$$\text{Langmuir}: q_e = \frac{K_L q_{max} C_e}{1 + K_L C_e} \quad \text{(S4)}$$

Where q_e (mg/g) and q_{max} (mg/g) represent the adsorption capacity of Gd(III) at equilibrium and the maximum adsorption capacity of PAMGO-3. C_e (mg/L) is the equilibrium Gd(III) concentration. K_L (L/mg) is the Langmuir constant related to affinity of binding sites and free energy of sorption. The data was fitted to the Langmuir model by plotting C_e/q_e against C_e, and the values of q_{max} and K_L were calculated from the slope and intercept.

$$\text{Freundlich}: q_e = K_F C_e^n \quad \text{(S5)}$$

Where K_F ($mg^{1-n}L^n/g$) and n are Freundlich constants and correlate to sorption capacity and sorption intensity, respectively. A linear plot was obtained by plotting lnq_e against lnC_e, and the values of K_L and n were calculated from the slope and intercept of the straight line.

$$\text{Temkin}: q_e = \frac{Rt}{b} lnK_t + \frac{Rt}{b} lnC_e \quad \text{(S6)}$$

Where K_t (L/g) and Rt/b (J/mol) are Temkin isotherm constants. R (8.314 J/mol. K) and t (298 K) are the gas constant and temperature, respectively.

SIII-4. Adsorption experiment and data fitting by kinetic models

The kinetic adsorption were conducted by adding 10 mg of PAMGO-3 into 50 mL solution with initial Gd(III) concentration was 50 mg/L at 298 K and pH of 5, the Gd(III) concentrations were determined by sampling at predetermined intervals in the time range of 1 to 60 min using ICP-OES method to analyze adsorption kinetics. For Gd(III) ion, the adsorbed concentration onto PAMGO-3 at time *t* can be measured as follow:

$$Q_t = \frac{(C_0 - C_t) \times V}{m} \tag{S7}$$

Where Q_t (mg/g) and C_t (mg/L) are the adsorption capacity and residual Gd(III) concentration in solution at different time.

To analyze the adsorption process of Gd(III) onto PAMGO-3, pseudo-first-order and pseudo-second-order kinetic models were used to fit the experimental kinetics data. The linear forms of the two models are expressed as follows:

$$\log(q_e - q_t) = \log q_e - \frac{k_1}{2.303} t \tag{S8}$$

$$\frac{t}{q_t} = \frac{1}{k_2 q_e^2} + \frac{t}{q_e} \tag{S9}$$

Where q_t (mg/g) and q_e (mg/g) are the adsorption capacity at time *t* and equilibrium, respectively. k_1 (min^{-1}) and k_2 ($gmg^{-1}min^{-1}$) represent rate constant of pseudo-first-order adsorption and pseudo-second-order model, respectively. The slope and intercept of log $(q_e\text{-}q_t)$ vs *t* and t/q vs *t*, respectively, were used to determine the

rate constants.

SIV. Recycling experiments

The recycling tests were conducted in six adsorption-desorption cycles. For the regeneration of PAMGO-3, which was achieved by dispersing the Gd(III)-loaded adsorbent into 50 mL of 0.5 M HCl solution for 10 h. After desorption, the solid was collected by centrifugation and the recovered adsorbent was dried before its reuse in the next cycle.

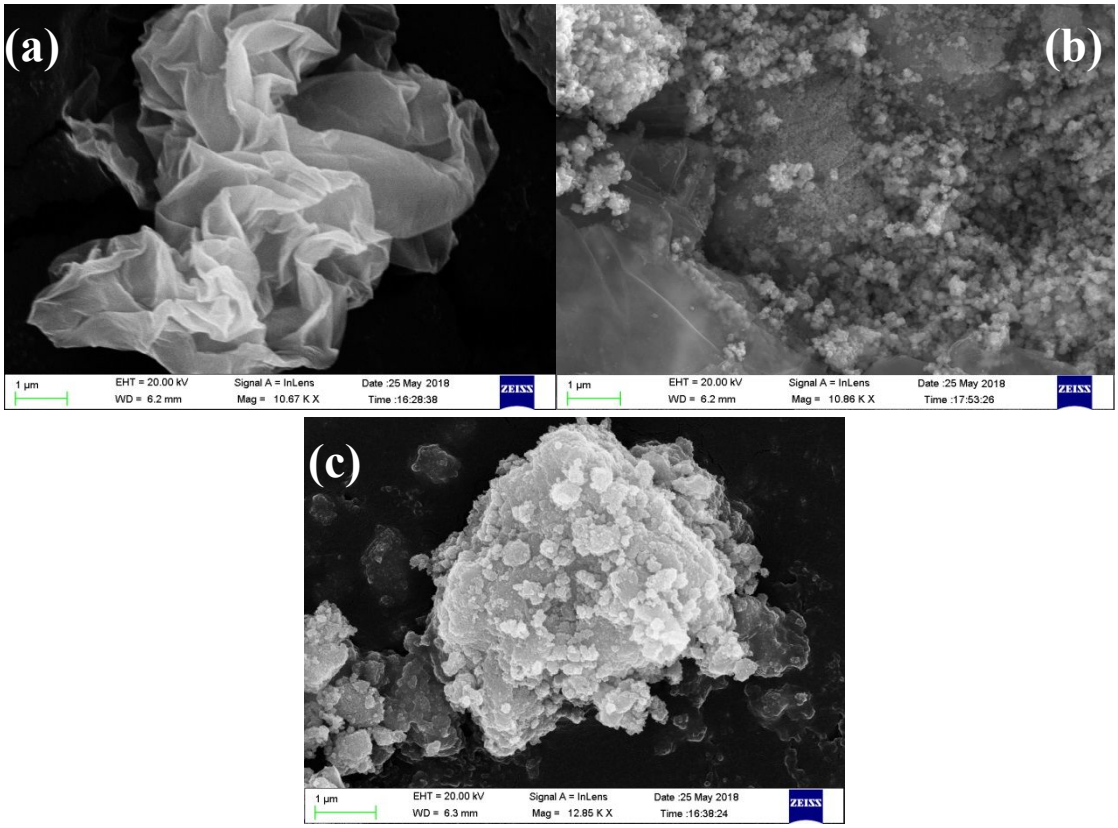

Figure S1 SEM images of GO (a); MGO (b); and PAMGO-3 (c).

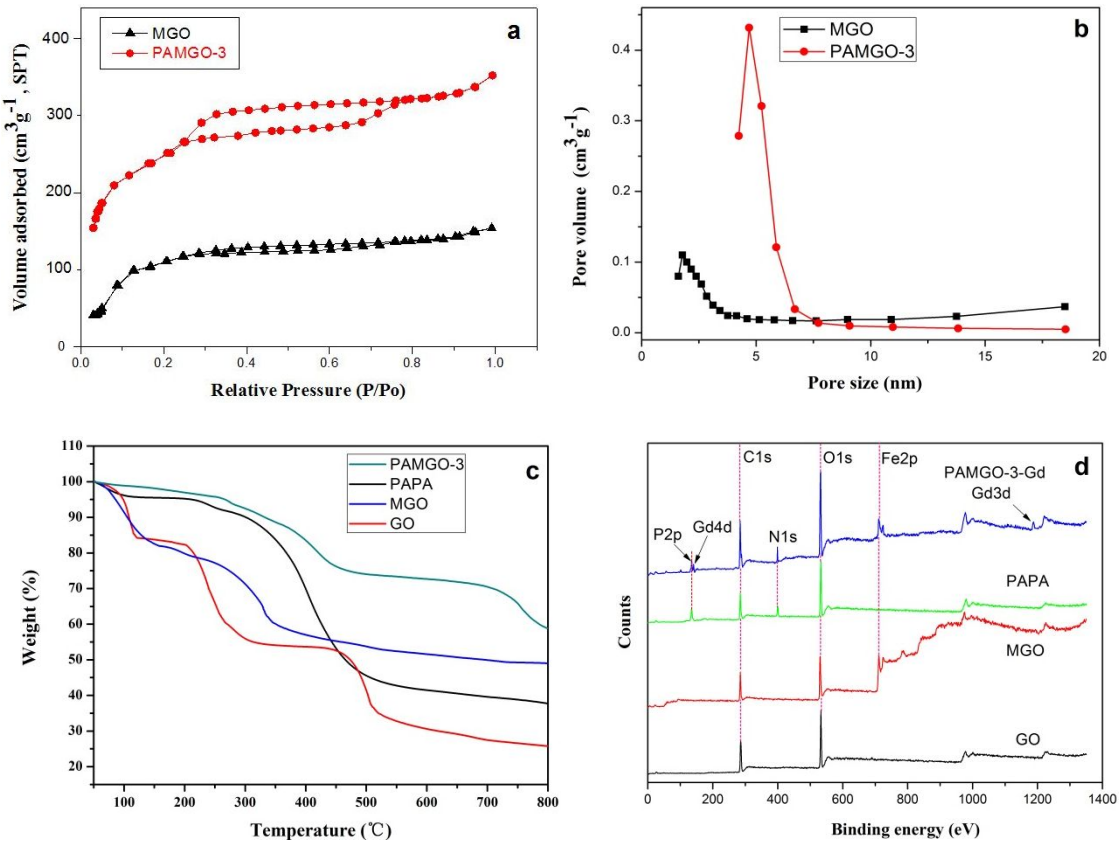

Figure S2 (a) Nitrogen adsorption-desorption isotherms and (b) Pore size distribution of MGO and PAMGO-3. (c) TGA curves of GO, MGO, PAPA and PAMGO-3. (d) XPS wide-scan of GO, MGO, PAMGO and PAMGO-Gd.

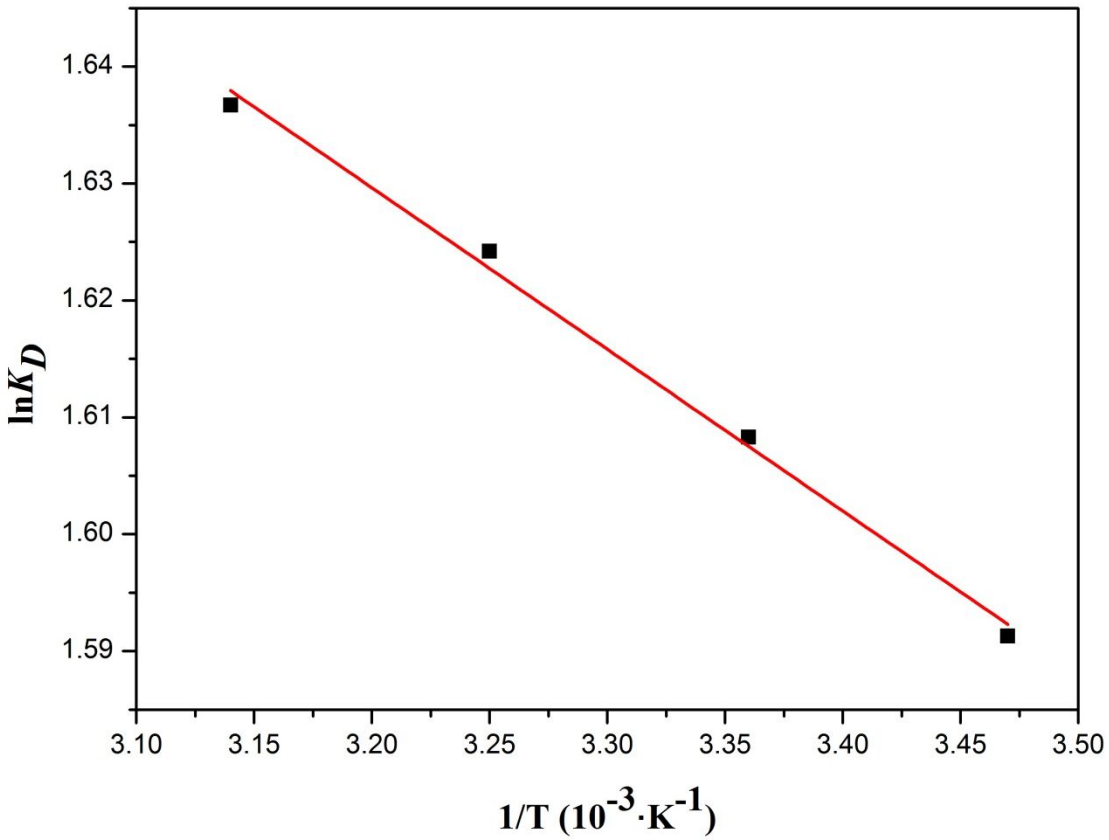

Fig. S3 Plot of lnK_D VS 1/T for the adsorption of Gd(III) by PAMGO-3 at varying temperature.

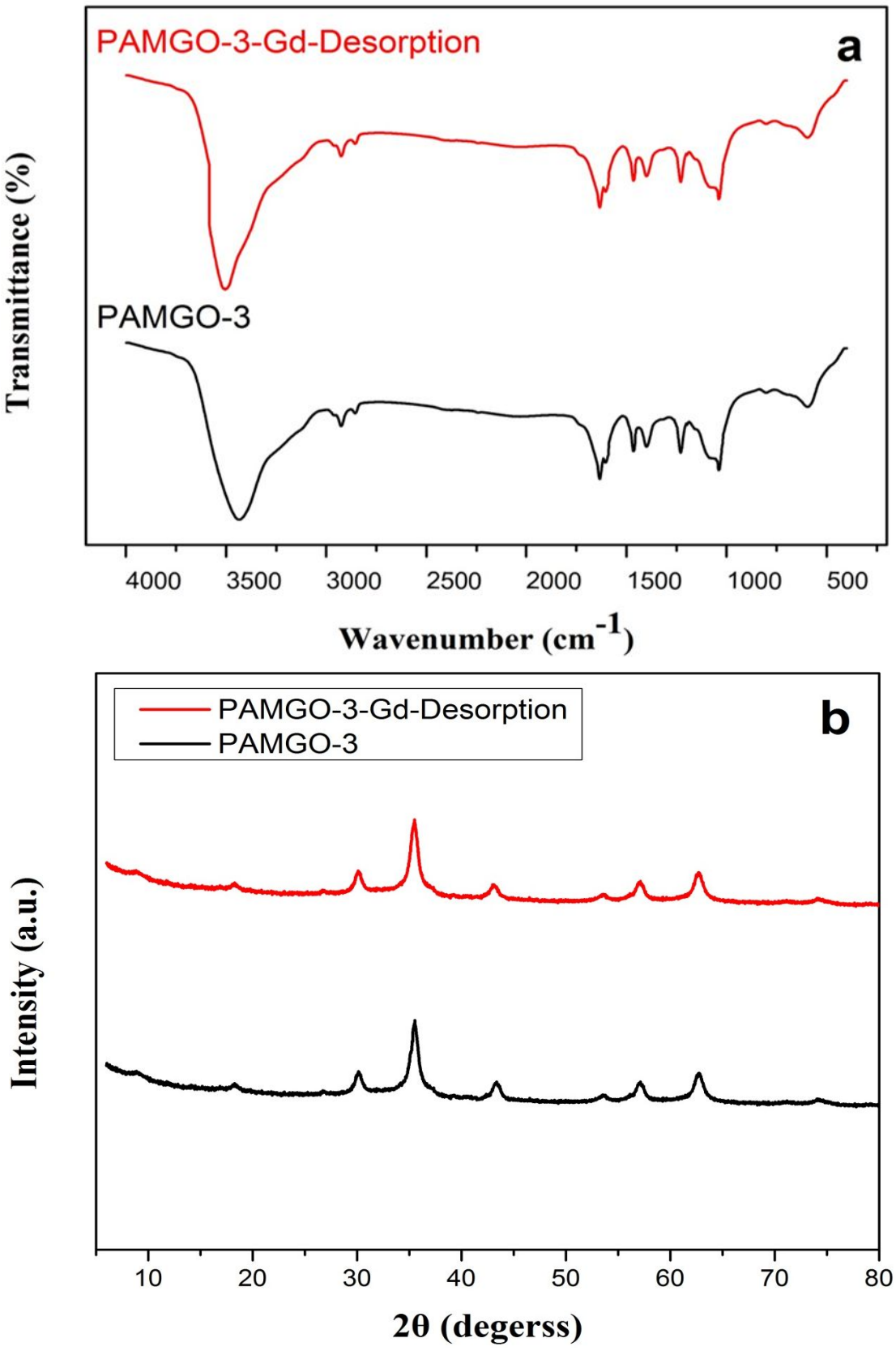

Figure S4 (a) FTIR spectra of PAMGO-3 and PAMGO-3-Gd-Desorption; (b) XRD patterns of PAMGO-3 and PAMGO-3-Gd-Desorption.

Table S1. The R_L values at 288, 298, 308 and 318 K with different initial concentrations.

C_0 (mg/L)	288K	298K	308K	318K
	R_L			
5	0.949	0.951	0.934	0.942
10	0.903	0.906	0.876	0.890
20	0.822	0.828	0.780	0.801
30	0.755	0.762	0.703	0.729
40	0.698	0.706	0.639	0.668
50	0.649	0.658	0.587	0.617
75	0.552	0.562	0.486	0.518
100	0.481	0.490	0.415	0.446
200	0.316	0.325	0.262	0.287

REFERENCES

(1) Li, N.; Yue, Q.; Gao, B.; Xu, X.; Kan, Y.; Zhao, P. Magnetic graphene oxide functionalized by poly dimethyl diallyl ammonium chloride for efficient removal of Cr(VI). *J. Taiwan. Inst. Chem. E.* **2018**, 91, 499-506.

(2) Chai, B. J.; Covina, W.; Muggee, F. D. Anaheim, both of Calif. **1980**, US Patent 4239695A.

(3) Langmuir, I. The adsorption of gases on plane surfaces of glass, mica and platinum. *J. Am. Chem. Soc.* **1918**, 143, 1361-1403.

(4) Freundlich, H. M. F. Over the adsorption in solution. *Zeitschrift fur Physikalische Chemie.* **1906**, 57, 385-470.

(5) Foo, K. Y.; Hameed, B. H. Insights into the modeling of adsorption isotherm systems. *Chem. Eng. J.* **2010**, 156, 2-10.